



Comparing two methods to estimate lateral force acting on stabilizing piles for a landslide in the Three Gorges Reservoir, China



Chunmei Zhou^{a,b,c,*}, Wei Shao^d, Cees J. van Westen^c

^a Institute of Rock and Soil Mechanics, Chinese Academy of Sciences, Wuhan 430071, China

^b School of Resource and Civil Engineering, Wuhan Institute of Technology, Wuhan 430073, China

^c Faculty of Geo-Information Science and Earth Observation (ITC), University of Twente, 7500 AE Enschede, The Netherlands

^d Water Resources Section, Faculty of Civil Engineering and Geosciences, Delft University of Technology, 2628 CN Delft, The Netherlands

ARTICLE INFO

Article history:

Received 6 September 2013

Received in revised form 13 February 2014

Accepted 15 February 2014

Available online 21 February 2014

Keywords:

Three Gorges Reservoir

Stabilizing piles

Hydrological models

Limit equilibrium method

Strength reduction method

Lateral force

ABSTRACT

Stabilizing piles are used worldwide to stabilize unstable slopes. However to date, there is little coverage in the scientific literature on the effects of the pore water pressure and the shear strength of the slip zone on the lateral force acting on the piles. This paper presents and compares two methods to estimate the lateral force acting on the stabilizing piles. These are the limit equilibrium method (LEM), and the finite element shear strength reduction method (FE-SRM). For both methods, the COMSOL software was used to model the infiltration of reservoir water and rainfall into the sliding mass. The distribution of lateral force was then simulated by the normal stress distribution on the piles with FE-SRM in PLAXIS 8.2 software. The effect of shear strength of the slip zone on the lateral force and its distribution were also studied. The lower Ercengyan landslide in the Three Gorges Reservoir was used as study area, with four different hydrological scenarios based on the reservoir water level fluctuations and rainfall amounts. The results show that the lateral force with the LEM method is slightly greater than with the FE-SRM method. The lateral force reaches a peak when the level of the reservoir rises to 175 m combined with high rainfall amount, and decreases linearly as the effective shear strength of the slip zone increases. The distribution of the lateral force is parabolic, and varies with the shear strength parameters of the slip zone. In conclusion, the LEM and FE-SRM methods can be used to calculate the lateral force acting on the stabilizing piles, and estimate the lateral force distribution. This technique effectively analyzes the behavior of stabilizing piles for landslides. It can be applied in the routine practical design of stabilizing piles in the Three Gorges Reservoir as well as other similar areas.

© 2014 Elsevier B.V. All rights reserved.

1. Introduction

The Three Gorges Project on the Yangtze River is the largest hydropower project in the world (Wu et al., 2011). The water table in the Three Gorges Reservoir is expected to change between 145 m and 175 m as a function of the annual flood intensity control. The water table fluctuations combined with heavy rainfall in this area have resulted in increased instability of the slopes (Cojean and Cai, 2011). To counteract this process, cast-in-place reinforced concrete piles have become a widespread and effective method to stabilize landslides in the Three Gorges Reservoir. Some successful applications of this technique have been reported in the literature (Ito and Matsui, 1975; Ito et al., 1981; Poulos, 1995; Chen and Poulos, 1997; Kim and Jeong, 2011; Lirer, 2012; Song et al., 2012).

Several methods have been published for calculating the lateral force acting on the piles in a landslide. Ito and Matsui (1975) developed the theory of plastic flow to estimate the lateral force. This model is used for rigid piles with infinite length and it is assumed that the soil around the piles is in plastic states, satisfying the Mohr–Coulomb's yield criterion. Hassiotis et al. (1997) extended the friction circle method to estimate the lateral force acting on the piles via the theory of elasticity. The friction circle method is limited to circular slip surfaces and homogeneous soil profiles. Recent advances in the lateral force are soil–pile interaction, which accounts for the influences of pile spacing, diameter, position, the capacity of piles and surrounding soils, interface roughness, soil dilation angle, and the shape of the soil arching (Kim and Jeong, 2011; Kourkoulis et al., 2011; Ashour and Ardalan, 2012). The lateral force transfer from moving soil to piles is observed and evaluated by different tests (Kahyaoglu et al., 2012). However, these methods are limited to homogenous soil slopes, and the geometry of the ground surface or slip surface is relatively regular with no special features (e.g. irregular ground surface or slip surface). In addition, these studies do not consider the effect of the pore water pressure and shear strength of the slip zone on the lateral force and its distribution.

* Corresponding author at: School of Resource and Civil Engineering, Wuhan Institute of Technology, Wuhan, China, 430073.

E-mail addresses: zhouchunmei@163.com, 2564937223@qq.com (C. Zhou), w.shao@tudelft.nl (W. Shao), c.j.vanwesten@utwente.nl (C.J. van Westen).

The most widely used method for evaluating slope stability and lateral force acting on the piles is still the limit equilibrium method (LEM) in conjunction with the method of slices in practical landslide engineering (Zhou and Cheng, 2013). This technique can accommodate complex slope geometries with variable soil properties, pore-water pressure conditions, different shapes of slip surfaces, and the influence of external boundary loads (Yamin and Liang, 2010). In the case of the Three Gorges Reservoir, the LEM allows the engineer to calculate the lateral force acting on the piles by using a desirable factor of safety for the pile–slope system while, at the same time, considering the level of the groundwater table changes due to heavy rainfall and water storage. However, the LEM only calculates the lateral force acting on the pile and not the distribution of lateral force, which directly affects the different lateral deflections, bending moment, and shear force for the pile.

The finite element model coupled with a shear strength reduction method (FE-SRM) is extensively used for comprehensive slope stability analysis. One of the advantages of the FE-SRM over the LEM is that no assumptions are needed about the shape and location of the critical failure surface. The location, shape, and magnitude of the plastic deformation area can be used to quantify the slip surface and factor of safety (Cheng et al., 2007). The lateral force acting on the pile can be obtained from the stress integration on the interface between the pile and the sliding soil above the slip surface, and its distribution can be derived from the stress distribution on the interface (Zhou, 2007).

It is generally recognized that slope stability is highly related to the subsurface hydrological processes in a hill slope (Gerscovich et al., 2006; Van Asch et al., 2006; Crosta and Frattini, 2008). Physically-based subsurface hydrological models are frequently integrated with slope stability analysis methods, such as the infinite slope stability analysis, limit

equilibrium slope stability analysis, and shear strength reduction method to calculate the safety factor and estimate which areas are susceptible for landslides (Crosta and Frattini, 2008).

This paper presents a simplified method to calculate the lateral force acting on the piles and obtain its distribution based on the LEM method and the FE-SRM method. The study area for the design and application of this method was a typical section of the Ercengyan landslide in Wanzhou District in China (Figure 1). First, the COMSOL Multiphysics® finite element software was used to model the hydrological processes of reservoir water table fluctuations from 145 m to 175 m in combination with intensive rainfall. The groundwater tables resulting from the hydrological modeling were used as input for the lateral force analysis. The lateral forces acting on stabilizing pile obtained from the LEM and FE-SRM models were then compared. In addition, the distributions of lateral force were obtained through the FE-SRM modeling. In this paper, the influence of reservoir water fluctuations, rainfall amounts and the shear strength of slip zone on the lateral force and its distribution are discussed. The methods to estimate lateral force for practical purposes are emphasized, and their applications are illustrated by site measurements.

2. Geological characteristics and stabilizing system of the Ercengyan landslide

2.1. Geometrical characteristics

The Ercengyan landslide is located in the Wanzhou District, near Chongqing City (Figure 1). The landslide is approximately 460 m in length (in the sliding direction), 530 m in width, $2.3 \times 10^5 \text{ m}^2$ in area,

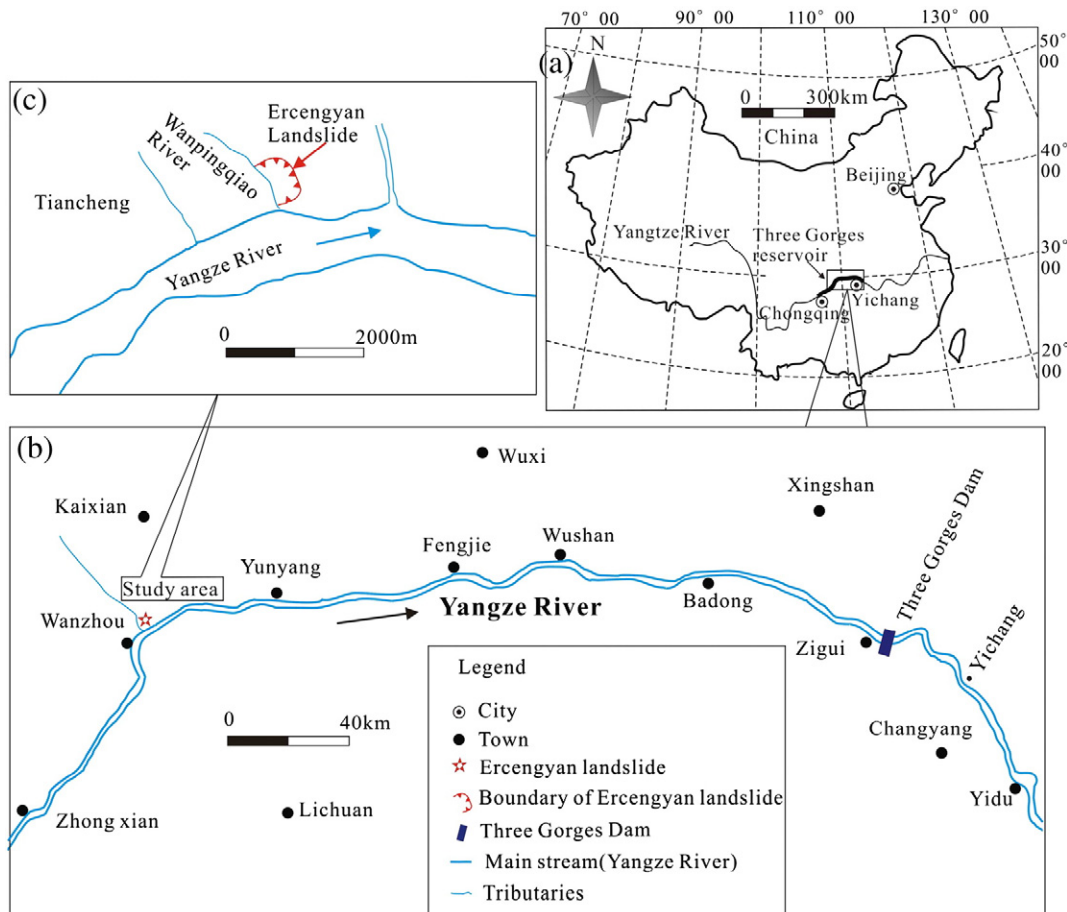


Fig. 1. (a) Location of the Three Gorges Reservoir; (b) Location of Wanzhou District along the Three Gorges Reservoir; (c) Ercengyan landslide used as the case study (indicated with a red arrow).



Fig. 2. (a) Photo of Ercengyan landslide and stabilizing piles; (b) Silty clay with gravels in the sliding soil (photo taken in 2002); (c) Striations on the slip surface from the shaft (2002); (d) Cast-in-place reinforced concrete piles (2006); (e) Reinforced concrete retaining wall inside pilehole (2006); (f) Top of a 3 × 4.5 m rectangular pile (2007).

and $3.80 \times 10^6 \text{ m}^3$ in volume. The landslide can be divided into two parts, each with different slope boundaries (Figure 2a). The upper landslide, located between 275 and 235 m, is an older landslide, which existed long before the construction of the Three Gorges reservoir. The lower landslide, located between 215 and 145 m, was re-activated after the construction of the Three Gorges dam and the rise of the lake level. The lower landslide is the study area in this paper (Figure 2a).

Geomorphological investigation shows that the Ercengyan landslide is a colluvial landslide that occurred in the Quaternary age. Examples of this type of landslide include the Xintan landslide (Chen, 1999), the Huanglashi landslide (Zhou et al., 2010), and the Jipazi landslide (Wei et al., 2006). This type of landslide is characterized by loose deposits, large pore volume, strong permeability, and large proportion of viscoplastic deformation. Statistical analysis shows that the colluvial landslides account for 17.73% of the total volume of landslides in the Three Gorges reservoir area (He et al., 2008).

2.2. Material and groundwater

The sliding mass is composed of gravel, silty clay, clay from the Quaternary landslide movement (Q_4^{del}), and residual deposits ($Q_4^{el} + el$) in the lower Ercengyan landslide. The gravel content is 20–30% and consists of argillaceous sandstone, sandstone and mudstones (Figure 2b). Most of the gravels are strongly weathered and easily broken. The materials in the slip zone consist of brown, gray-yellow, and gray-white silty clays with some gravel. The slip surface and striations can be clearly seen from the vertical shafts made on the landslide (Figure 2c). The bedrock consists of siltstone and mudstone from the Jurassic Shaximiao Formation (J_2s) with an average dip direction of 340° and a dip angle of $4\text{--}5^\circ$. The bedrock near the surface is strongly weathered, with a thickness ranging between 0.2 and 19.7 m, and an average thickness of 5.0 m. The original groundwater table was determined by measuring the depth of the water in the boreholes in 2002, and varied between 4.5 and 8.5 m below the ground surface (Figure 3b).

2.3. Shear strength of slip zone

Numerous research projects have determined the shear strength parameters cohesion c and friction angle Φ of the slip zone in the Three Gorges area (Huang, 2004; Wen et al., 2007). The friction angle of the

slip zone Φ decreases with increasing clay content (Wen et al., 2007), and increases with increasing gravel content (Li et al., 2008). The shear strength decreases significantly as the slip zone saturates (Jian et al., 2007). The distribution form of c follows a logarithmic normal distribution, and ranges between 5–42 kPa (saturated residual state). The friction angle Φ follows a normal distribution, ranging between 3.7 and 16.5° (saturated residual state) (Luo et al., 2005).

Further measurements were collected of the shear strength of the slip zone from other stabilized landslides (e.g. Wangjiang road landslide, Dou Yapeng landslide, and Pipaping landslide) in the Wanzhou District. Based on these data, the cohesion c is between 15–45 kPa (nature state) and 12.4–40 kPa (saturated state). The friction angle Φ varies between $11.5\text{--}20^\circ$ (nature state) and $10.5\text{--}18^\circ$ (saturated state) (Yu, 2005).

Data on the effective shear strength of the slip zone (saturated state) in the lower Ercengyan landslide were obtained from shear tests of samples of the slip zone (Table 1). The other parameters of the soil and rock are also shown in Table 1, which were obtained from site investigation and associated laboratory tests (Yu, 2005).

2.4. Slope stabilization system

Piles used to stabilize landslides now constitute 78% of all prevention measures for landslides in the Wanzhou District. The piles are mostly rectangular in shape with a size relation of $1.5 \times 2 \text{ m}$, $1.5 \times 2.5 \text{ m}$ or $2.0 \times 3.0 \text{ m}$. The spacing of piles ranges between 5 and 10 m, and the most common spacing is 5 m or 6 m. The depth of piles ranges between 9 and 50 m. The ratios of the embedment depth in the stable stratum to the total pile depth range between $1/4\text{--}1/2$, and most frequently are $1/3$ (Zhou, 2007).

The Ercengyan landslide was stabilized using a series of stabilizing piles located at an elevation of 175 m and drainage ditches both along the landslide boundaries and inside the landslide (Figures 2d–f, 3a). Construction began in June 2006 and ended six months later. Five different sizes of cast-in-place reinforced concrete piles were used (indicated as A to E in Figure 3a). These different pile sizes were implemented as a result of calculations that showed that different lateral forces were acting on the piles in different sections of the landslide. In this paper, the lateral force acting on the pile at Section 2-2 in the lower Ercengyan landslide is estimated. Details of the procedure and the implementation process are presented in Fig. 4.

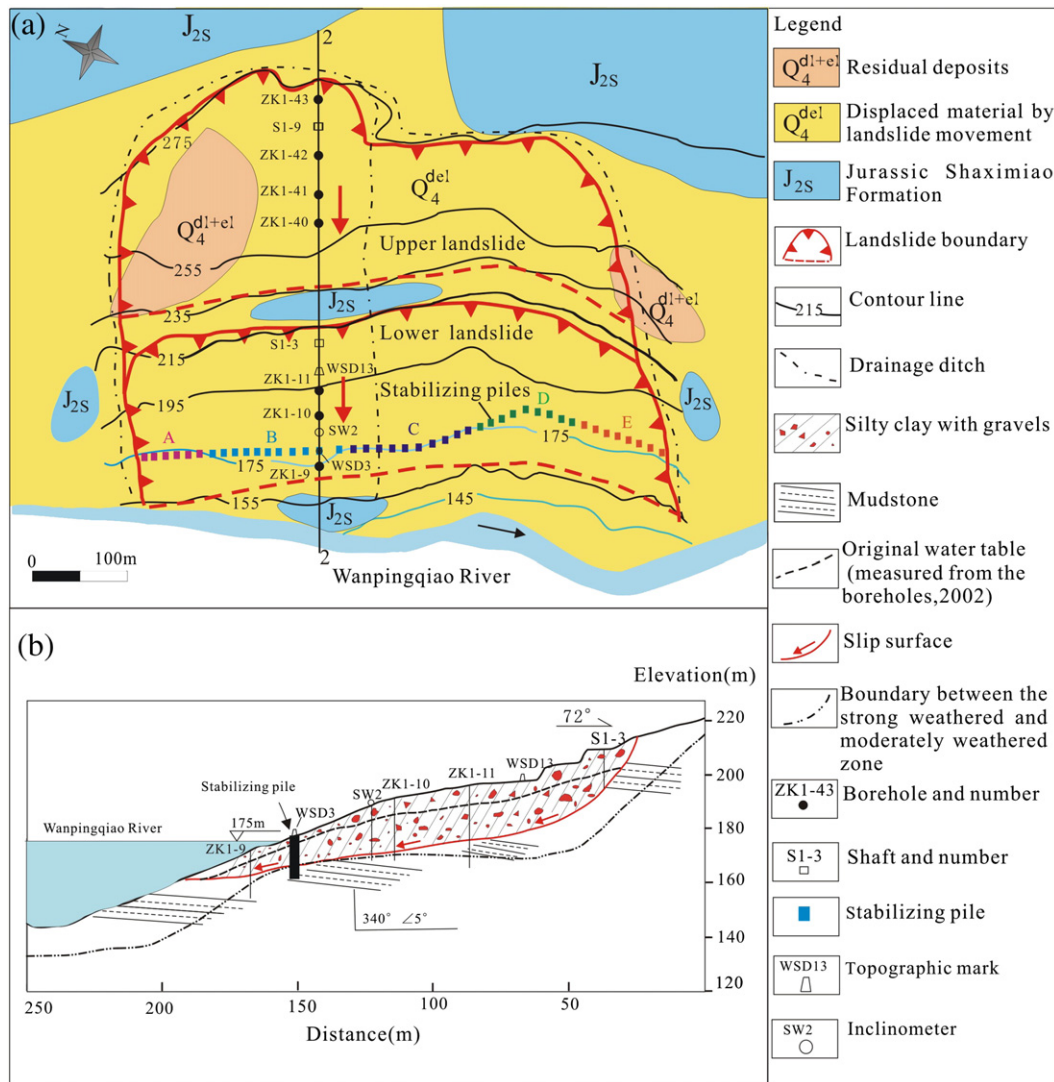


Fig. 3. (a) Geological map of the Ercengyan landslide; (b) Geological profile of Section 2-2 in the lower Ercengyan landslide and in situ monitoring instruments indicated in Fig. 3a.

2.5. Field measurements

To observe the behavior of the soils and the piles, a series of in situ monitoring instruments with topographic markers and inclinometers were installed in Section 2-2 in January 2007 (see Figure 3b). The two topographic markers were designed to monitor the deflections of the surface soil and the pile. One was placed on the ground surface between the scarp and the pile, and the other was installed on the pile top. Inclinometers, placed in the slip zone nearby the pile, observed the displacement of soil near the surface. The monitoring data from Jan 2007 to Nov 2009 shows that the deflections of the surface soil and pile are no more than 15 mm, and the deflection of the slip zone is about 5 mm. The movements were very small, indicating that the Ercengyan landslide remained stable after the construction of the piles.

3. The hydrological process within the Ercengyan landslide

3.1. Rainfall conditions

Many landslides have been triggered by heavy rainfall, such as the Tiantaixiang landslide (Huang, 2004), the Minguochang landslide (Jian et al., 2005, 2007), the Qianjiangping landslide (Zhang et al., 2004; Liao et al., 2005), and the Huangtupo landslide (Cojean and Cai, 2011). The effects of rainfall infiltration and the behavior of the stabilizing piles have been analyzed based on in situ measurements (Song et al., 2012).

Wanzhou is located in the mid-latitude zone, and experiences heavy precipitation. The average annual rainfall amount is 1253 mm, with the largest annual rainfall, 1635.2 mm, recorded in 1982 (Jian et al., 2009). The rainy season mostly occurs from May to September, and accounts

Table 1
Soil and rock properties. Source: Yu (2005).

Material	Unit weight γ (kN/m ³)		Young's modulus E (kN/m ²)	Poisson's ratio ν	Effective cohesion c (kPa)	Effective friction angle ϕ (°)	The strength reduction factor for interfaces R_{inter}
	Dry	Saturated					
Soil (gravel, silty clay and clay)	22	22.4	30	0.3	32.7	15.6	0.7
Slip zone (silty clays with some gravel)	22	22.4	30	0.3	21.7	14.6	0.65
Bedrock (siltstone and mudstone)	25	25.3	1.1×10^3	0.25	300	33	0.7

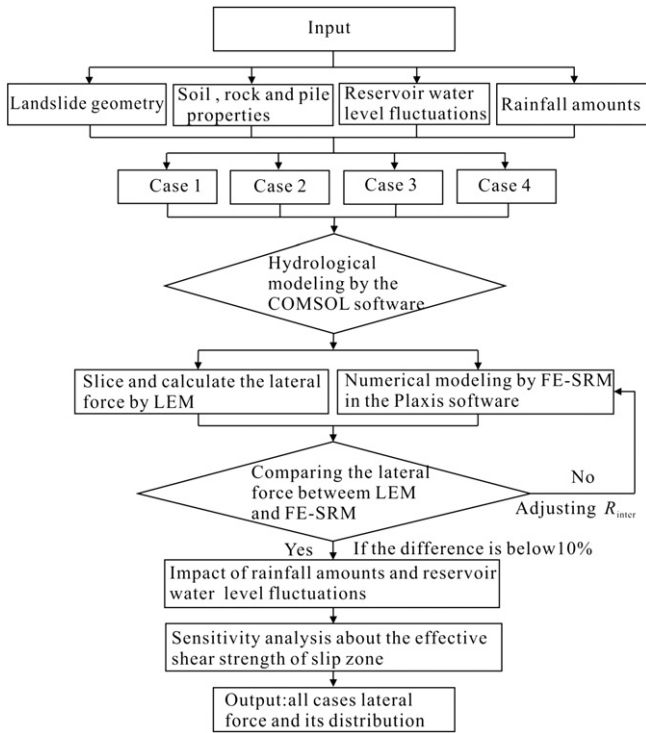


Fig. 4. The procedure and implementation process for lateral force acting on the piles.

for 60–70% of the total annual rainfall. In the period from 2007 to 2009, the highest monthly rainfall was 293.6 mm in July 2008 (Figure 5).

Landslides are, for the most part, caused by a rise in the groundwater table, occurring after a rainfall event. Therefore, for the simulation in this study, a hypothetical time of 30 days was used for the groundwater modeling based on the monthly average rainfall. The 30-days hypothetical time was selected to allow for the infiltrated rainfall to reach the groundwater table. A low rainfall amount was considered to be 150 mm with a rainfall intensity of 5 mm/day during a 30-day period. A high rainfall amount was considered to be 360 mm with a rainfall intensity of 12 mm/day during a 30-day period. Since the actual monthly average rainfall amount should subtract evaporation from the average rainfall amount, the evaporation rate is assumed to have a constant value of 2.8 mm/day (Qiao, 2012).

3.2. Reservoir water level fluctuation

Many landslides have been triggered or reactivated by the rising water level of reservoirs, for example, the catastrophic Vaiont reservoir

slide in 1963 in Italy (Hendron and Patton, 1987; Alonso and Pinyol, 2010). Water level fluctuation has an important impact on the hydrological conditions of the slope, particularly the properties of the sliding soil, slip zone, and under water bedrock (Jian et al., 2005; Zhou, 2007). Similarly, the annual variation of water level seriously impacts the slope stability and the lateral forces on the stabilizing piles (Wu et al., 2001).

The water level of the Three Gorges Reservoir fluctuated between 135 and 156 m from June 2006 to June 2008 (during construction of the reservoir dam), and has fluctuated between 145 and 175 m from June 2008 to Dec 2013. The lower 135 m level was only observed during the construction of the reservoir, rising to 145 m after the dam completion. The reservoir level is lowered every year during the rainy season from May to September (Figure 6), buffering against a large inflow of water in the case of major rainfall in the upper catchment.

To design stabilizing piles for the Ercengyan landslide, three water level scenarios in the Three Gorges Reservoir were considered: 145 m (flood period), 175 m (storage period) and lowering from 175 m to 145 m (water supply period).

3.3. Physically-based subsurface hydrological models

Both the rainfall and fluctuation of the Three Gorges Reservoir water level significantly influences the effective stress of the soil particles and lateral force acting on the pile. The combined effect of rainfall and reservoir water level on changes in subsurface flow was simulated using the COMSOL Multiphysics® finite element software (Comsol, 2013).

In the Subsurface Flow module of the COMSOL, the two-dimensional vertical and horizontal flow was described by the Richards Equation. The Brooks–Corey model (Brooks and Corey, 1964) was used for the sliding soil hydraulic function. The sliding soil was divided into two layers, the upper soil and the lower soil (Yu, 2005). The saturated hydraulic conductivity K_s of the upper soil was 6.13×10^{-7} m/s, and the lower soil was 3.5×10^{-8} m/s. The other parameters for the Brooks–Corey model in COMSOL can be found in Table 2 and the literature (Rawls et al., 1982).

The initial boundary conditions for the COMSOL hydrological analysis are as follows (Figure 7a). The rainfall infiltration and seepage boundary conditions were similar to the ones in the study by Chui and Freyberg (2009). The interface of the soil and bedrock was defined as a no-flux boundary condition, and the bedrock was assumed to be impermeable. The submerged area of the slope under the storage scenario was defined as the pressure head boundary condition, and the static reservoir water pressure was loaded onto the submerged area of the slope. The surface that receives rainfall and evaporation was defined as the atmospheric boundary, and the actual infiltration or evaporation rate depended on the surface pore water pressure. The initial phreatic

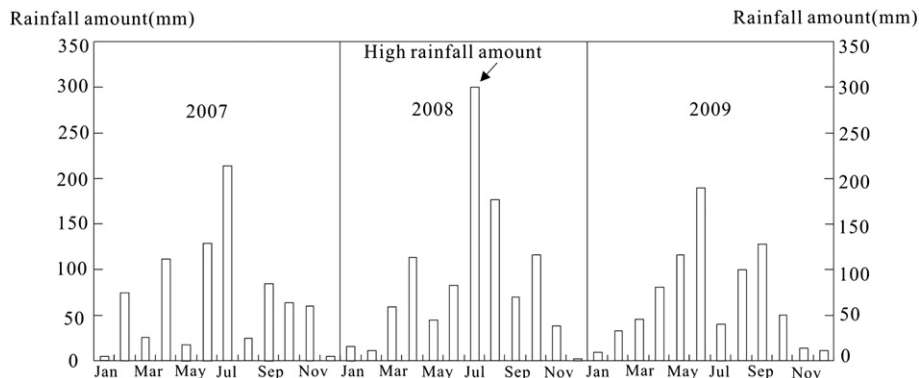


Fig. 5. Monthly rainfall amount in Wanzhou District from 2007 to 2009. Source: <http://www.cjxx.cn>.

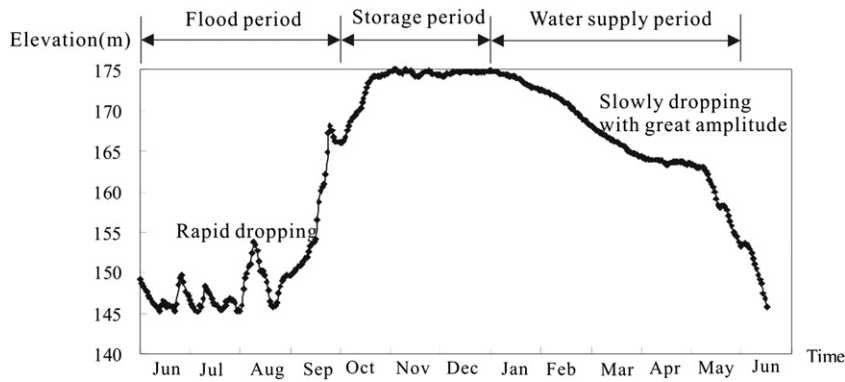


Fig. 6. Fluctuation of the reservoir water level near Wanzhou District since June 2008.

Source: <http://www.cjxt.cn/>.

surface was considered as the original groundwater table, which was based on field measurements from a series of boreholes (see Figure 3b).

3.4. Hydrological scenarios

During the flood period, the low reservoir water level is usually sustained at 145 m, and rainfall amount is usually high. In the storage period, the reservoir water level is usually sustained at 175 m, and both low and high rainfall amounts are considered. The 175 m water level dropdown to 145 m is usually associated with low rainfall amounts. Therefore, the following four hydrological scenarios were used for the groundwater modeling:

- Case 1 145m water level + rainfall amount of 360 mm/30-days;
- Case 2 175m water level + rainfall amount of 150 mm/30-days;
- Case 3 175m water level + rainfall amount of 360 mm/30-days;
- Case 4 175m water level dropdown to 145 m water table + rainfall amount of 150 mm/30-days.

The groundwater levels for the four scenarios are shown in Fig. 7b. The results show that the rainfall amounts have more influence on the groundwater level than the lake water variations. When the lake is at a low water level of 145 m (case 1), the high rainfall amount leads to saturation in a large part of the landslide. The same saturation exists for case 3, when the lake rises to the highest water level of 175 m. The groundwater tables from the four scenarios were used as input for the slope stability analysis and the lateral force estimation in the LEM and FE-SRM methods.

4. Lateral forces acting on the stabilizing piles

4.1. Calculating lateral forces with the LEM method

The LEM method was developed by experienced engineers in China and is widely used for geological disaster prevention in the Three Gorges Reservoir and other geotechnical designs. The following assumptions were applied to the LEM when analyzing the lateral forces

Table 2
The parameters for the Brooks–Corey model in COMSOL.

Parameter	Silty clay with gravel
Residual water content θ_r	0.056
Saturated water content θ_s	0.42
Saturated hydraulic conductivity of upper soil K_s (m/s)	6.13×10^{-7}
Saturated hydraulic conductivity of lower soil K_s (m/s)	3.5×10^{-8}
Fitting parameter α (1/m)	2.9
Fitting parameter n	0.13
Fitting parameter l	1

acting on the stabilizing piles: (1) The plane strain model is applicable in the lateral force analysis; (2) The sliding soil is a rigid body divided into a series of vertical slices and it slides along a particular polygonal

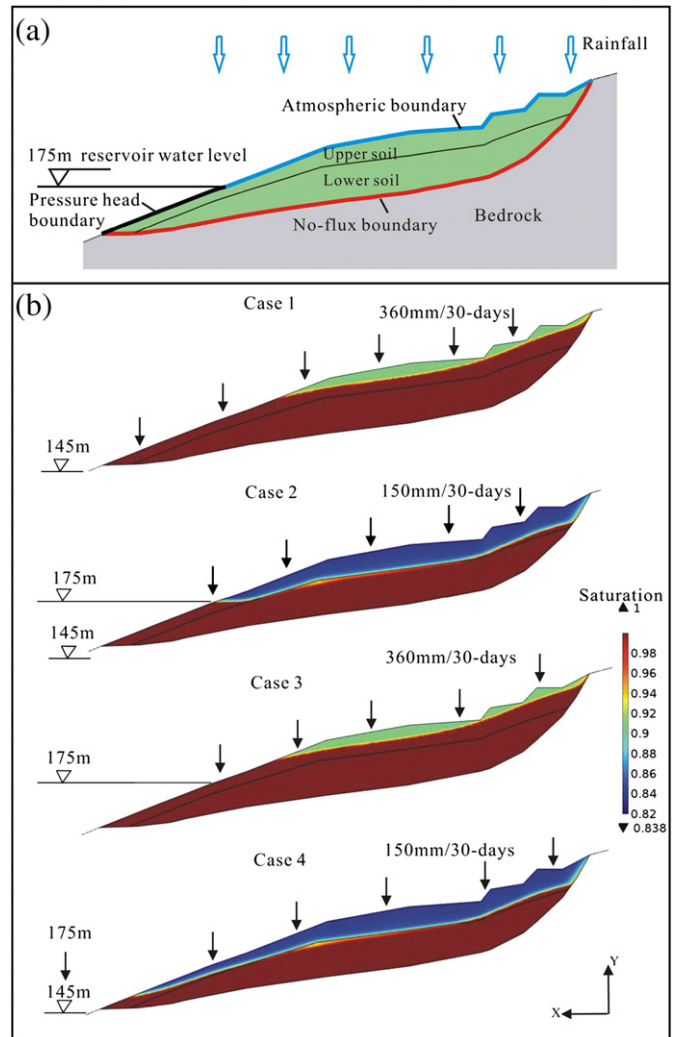


Fig. 7. (a) The initial boundary conditions for COMSOL analysis. The green is geological map of the soil, and the gray is the bedrock; (b) The saturation with different rainfall and reservoir water levels by COMSOL modeling. The brownish red is the saturated zone, and the water content of unsaturated zone can be approximated to be a constant value.

slip surface (Figure 8); (3) The force equilibrium of all slices is satisfied; (4) The Mohr–Coulomb's yield criterion is applied; (5) If the resultant of interslice force E_i (parallel to the slip surface) is negative, the value is assumed to be zero.

Based on Robert (1999) and Yamin and Liang (2010), we developed the following equations. The pore water pressure using seepage forces and buoyant unit weight are considered for a typical slice i , in both perpendicular (Eq. (1)) and parallel directions (Eq. (2)) to the base of each slice.

$$N_i = (Q_i + W_{i1} + W_{i2}) \cos \theta_i - D_i \sin(\theta_i - \alpha_i) + E_{i-1} \sin(\theta_{i-1} - \theta_i) \quad (1)$$

$$T_i = (Q_i + W_{i1} + W_{i2}) \sin \theta_i + D_i \cos(\theta_i - \alpha_i) + E_{i-1} \cos(\theta_{i-1} - \theta_i) - E_i \quad (2)$$

where N_i is the force normal to the base of slice i (kN), T_i is the force parallel to the base of slice i (kN), Q_i is the external surcharge applied at slice i (kN), W_{i1} is the weight of slice i above the water table (kN), $W_{i1} = \gamma V_{i1}$, γ is unit weight of soil (kN/m³), V_{i1} is the volume of the slice i above the water table (m³), W_{i2} is the buoyant weight of slice i below the water table (kN), $W_{i2} = \gamma' V_{i2}$, γ' is buoyant unit weight of soil (kN/m³), V_{i2} is the volume of the slice i below the water table (m³), θ_i is the inclination of slice i base ($^\circ$), θ_{i-1} is the inclination of slice $i-1$ base ($^\circ$), α_i is the inclination of the internal water table of slice i ($^\circ$), E_{i-1} is the interslice force of slice $i-1$ (kN), E_i is the interslice force of slice i and the lateral force acting on the pile for a 1 m-width of sliding soil (kN).

The seepage force D_i acting in the direction of the flow line ef (as seen in Figure 8b) can be calculated as follows (Craig, 1987):

$$D_i = i \gamma_w V_{i2} \quad (3)$$

where i is the average hydraulic gradient across the slice, $i = \sin \alpha_i$, γ_w is the unit weight of water (kN/m³), V_{i2} is the volume of the slice i below the water table (m³), if the slice is under the water level (Figure 8c), then $D_i = 0$, $Q_i = 0$, $W_{i1} = 0$ and $W_{i2} = \gamma' V_i$, where V_i is the total volume of slice i (m³).

The lateral force E_i can be developed on the basis of Yamin and Liang (2010) as follows:

$$E_i = A_i + \sum_{n=1}^{i-1} A_n \prod_{j=n+1}^i B_j \quad (4)$$

$$A_i = D_i \cos(\theta_i - \alpha_i) + (Q_i + W_{i1} + W_{i2}) \sin \theta_i - \frac{c_i L_i}{F_s} \tan \phi_i + [D_i \sin(\theta_i - \alpha_i) - (Q_i + W_{i1} + W_{i2}) \cos \theta_i] \frac{\tan \phi_i}{F_s} \quad (5)$$

$$B_j = \cos(\theta_{j-1} - \theta_j) - \frac{\sin(\theta_{j-1} - \theta_j) \tan \phi_j}{F_s} \quad (6)$$

where c_i is the slip zone effective cohesion at the base of slice i (kPa), ϕ_i is the slip zone effective friction angle at the base of slice i ($^\circ$), L_i is the length of the base of slice i (m), F_s is the desired slope safety factor, which is determined by landslide classification, load combinations, and the fluctuating of water table in the reservoir (Xu, 2012).

The following empirical formula is used to estimate the lateral force E for design of the pile, with each pile having center-to-center spacing l (Hassiotis et al., 1997).

$$E = E_i l \cos \theta_i \quad (7)$$

In this paper, we focus on the study of the lateral force E_i . The shear resistance R_{i+1} of the sliding soil before the stabilizing pile was determined by the lowest value of the resistance force and passive earth pressure of the soil (Waltham, 1994). However, in the practical design of stabilizing piles in the Three Gorges Reservoir, the shear resistance, R_{i+1} , was considered to be equal to zero when the sliding soil before the pile was unstable due to the rising of the reservoir level or high rainfall amount (Xu, 2012).

The slope safety factor F_{s1} without stabilizing piles was obtained by Eq. (8). The slope safety factor F_{s1}' with the piles, Eq. (9), was derived using E_i from Eq. (4) and assuming that only the lateral force is acting on the pile.

$$F_{s1} = \frac{\sum_{i=1}^n (N_i \tan \phi_i + c_i L_i)}{\sum_{i=1}^n T_i} \quad (8)$$

$$F_{s1}' = \frac{\sum_{i=1}^n (N_i \tan \phi_i + c_i L_i) + E_i}{\sum_{i=1}^n T_i} \quad (9)$$

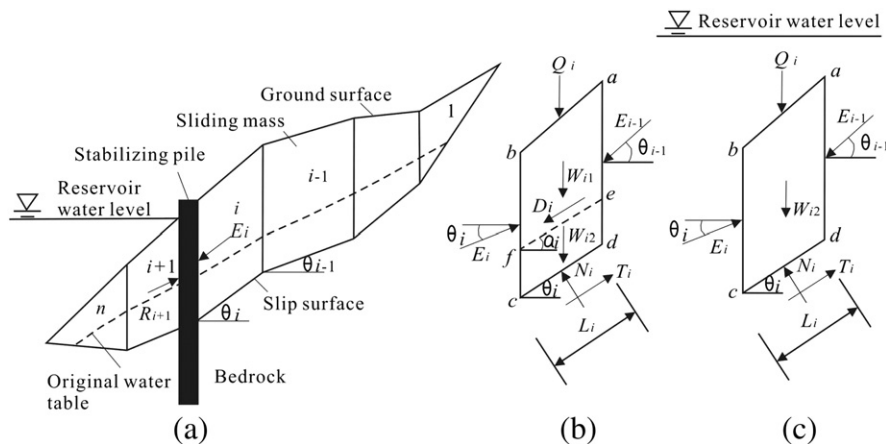


Fig. 8. Schematic representation of the LEM method. (a) Sliding soil divided into n vertical slices; (b) External forces acting on a typical slice i with the internal water table; (c) External forces acting on a typical slice i with the external water table.

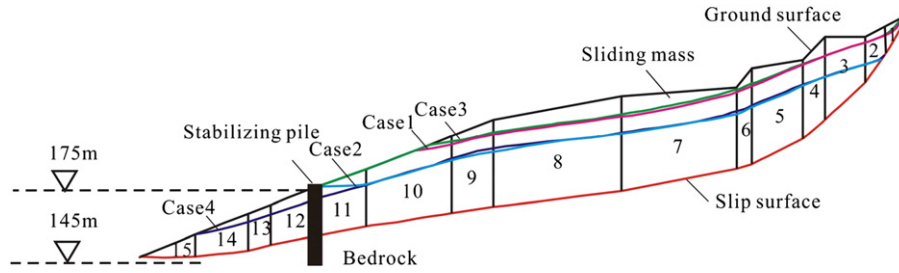


Fig. 9. Profile of the lower Ercengyan slope 2-2 section with indication of the slices, pile and groundwater levels modeled for the different scenarios (see Figure 7).

Eqs. (4), (8), and (9) are useful equations that enable engineers to determine the slope safety factor and the lateral force acting on the stabilizing piles. The reason why this method is popular in China is that it is simple to use and has been proved effective for pile design, considering the desired safety factor for each case is F_s . However, the LEM method in this paper does not consider the moment equilibrium. If the LEM method is used in another country, one should check the results carefully and compare them with the rigorous limit equilibrium techniques that satisfy both force and moment equilibrium, such as those studied by Janbu (1954), Morgenstern (1965), Spencer (1967) and others.

4.2. Calculating the lateral forces with the FE-SRM

Owing to the shortage of the distribution of lateral force in the LEM method, the lateral force was also analyzed using the FE-SRM method. A two-dimensional finite element program PLAXIS 2D (version 8.2) was used to model a single pile in Section 2-2 in the lower Ercengyan landslide (Figure 3). The shear strength reduction method SRM, called the *Phi-c reduction* approach in PLAXIS (Brinkgreve and Vermeer, 2002), has been used in both the analysis of the slope safety factor without piles (Griffiths and Lane, 1999; Cheng et al., 2007, 2008), and the slope safety factor with piles (Won et al., 2005). However, few works

have used the FE-SRM methods on the lateral force acting on the pile and its distribution.

The lateral force acting on the stabilizing pile is the area of the normal stress diagram (Budhu, 1999), which is:

$$E_A = \int_0^{H_0} \sigma_n dz \tag{10}$$

where σ_n is the normal stress acting on the interface of the pile and soil above the slip surface (kPa), and H_0 is the length of the pile above the slip surface (m).

According to the result by Zheng and Zhao (2004), one can calculate the distribution of the lateral force acting on the pile by comparing the lateral force between Eqs. (4) and (10), E_i and E_A . If the $E_i \approx E_A$, the distribution of σ_n is the distribution of the lateral force. If the $E_i \neq E_A$, then one must adjust the R_{inter} (the interface strength reduction factor) (Brinkgreve and Vermeer, 2002) of the slip zone until the difference between E_i and E_A is below 10%.

The two-dimensional modeling by the FE-SRM method cannot consider the influence of pile spacing l to the lateral force E_A . Therefore, this paper can only obtain the lateral force and its distribution for every 1 m-width sliding soil, and use the empirical formula (7) to estimate the lateral force E for designing the pile.

5. Applying the LEM and FE-SRM method in the Ercengyan landslide

5.1. The lateral force calculated by the LEM method

The slices of Section 2-2 in the lower Ercengyan landslide with a stabilizing pile are shown in Fig. 9. The sliding soil is divided into 15 vertical slices according to the ground surface morphology. The stabilizing pile is located behind slice 11. The desired slope safety factor F_s is 1.15 (Yu, 2005).

By solving Eqs. (4), (8), and (9), one can calculate the slope safety factor F_{s1} without the pile and F_{s1}' with the pile, and the lateral force E_{11} acting on the pile in four cases (see Table 4). The following comments can be made.

The slope safety factor F_{s1} without the pile is greatly affected by the rainfall amounts and nominally changes as the reservoir water level

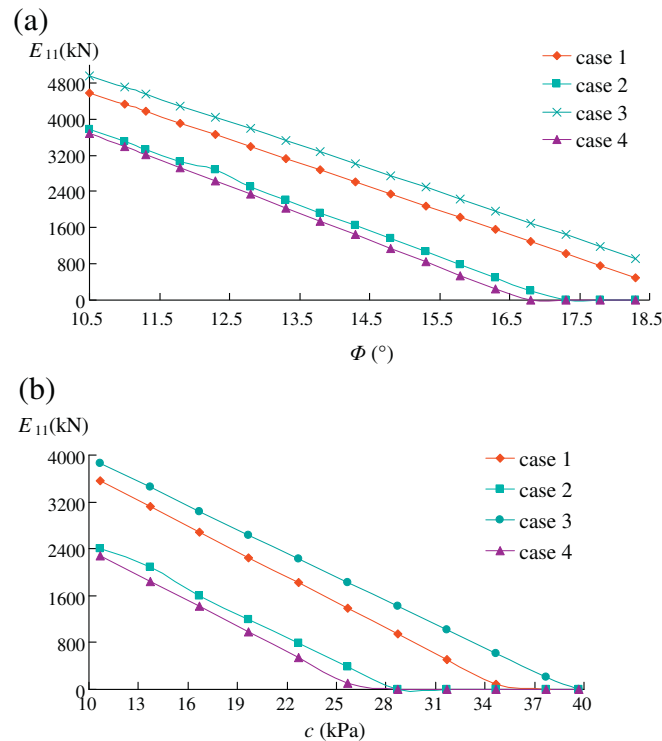


Fig. 10. Sensitivity analysis between the lateral force E_{11} and the effective shear strength of slip zone. (a) when cohesion $c = 21.7$ kPa; (b) when friction angle $\phi = 14.6^\circ$.

Table 3
Pile material data sets for plate in PLAXIS.

Parameter	Pile
Young's modulus E (kN/m ²)	3×10^7
Axial stiffness per unit width in the out-of-plane direction EA (kN/m)	2.25×10^8
Flexural rigidity per unit width in the out-of-plane direction EI (kN m ² /m)	1.69×10^8
Weight per unit area w (kN/m/m)	24
Poisson's ratio ν	0.2
Pile size, $a \times b$ (m) (a is out-of-plane direction)	2.5×3
Pile depth (m)	17
Pile embedment depth in the bedrock (m)	6.6

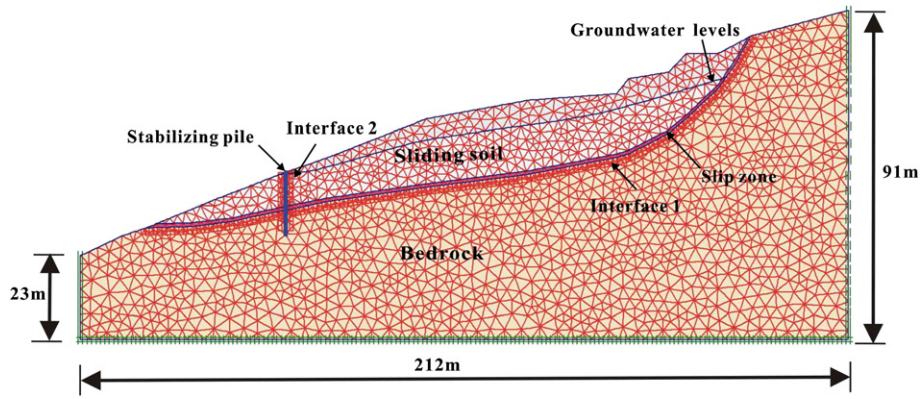


Fig. 11. Numerical model of Ercengyan landslide for FE-SRM analysis.

changes. F_{s1} is larger than 1.0 in cases 2 and 4 (small rainfall), and almost reaches 1.0 under cases 1 and 3 (high rainfall). For example, when the level of the reservoir rises to 175 m, F_{s1} is reduced from 1.12 (a small rainfall amount, case 2) to 1.01 (a high rainfall amount,

case 3). Therefore, the slope will lose stability due to the high rainfall amount if no control measures are taken. This result is consistent with the statistical data, which indicates that 83% of the total landslides in the Three Gorges Reservoir happen in periods of high rainfall between

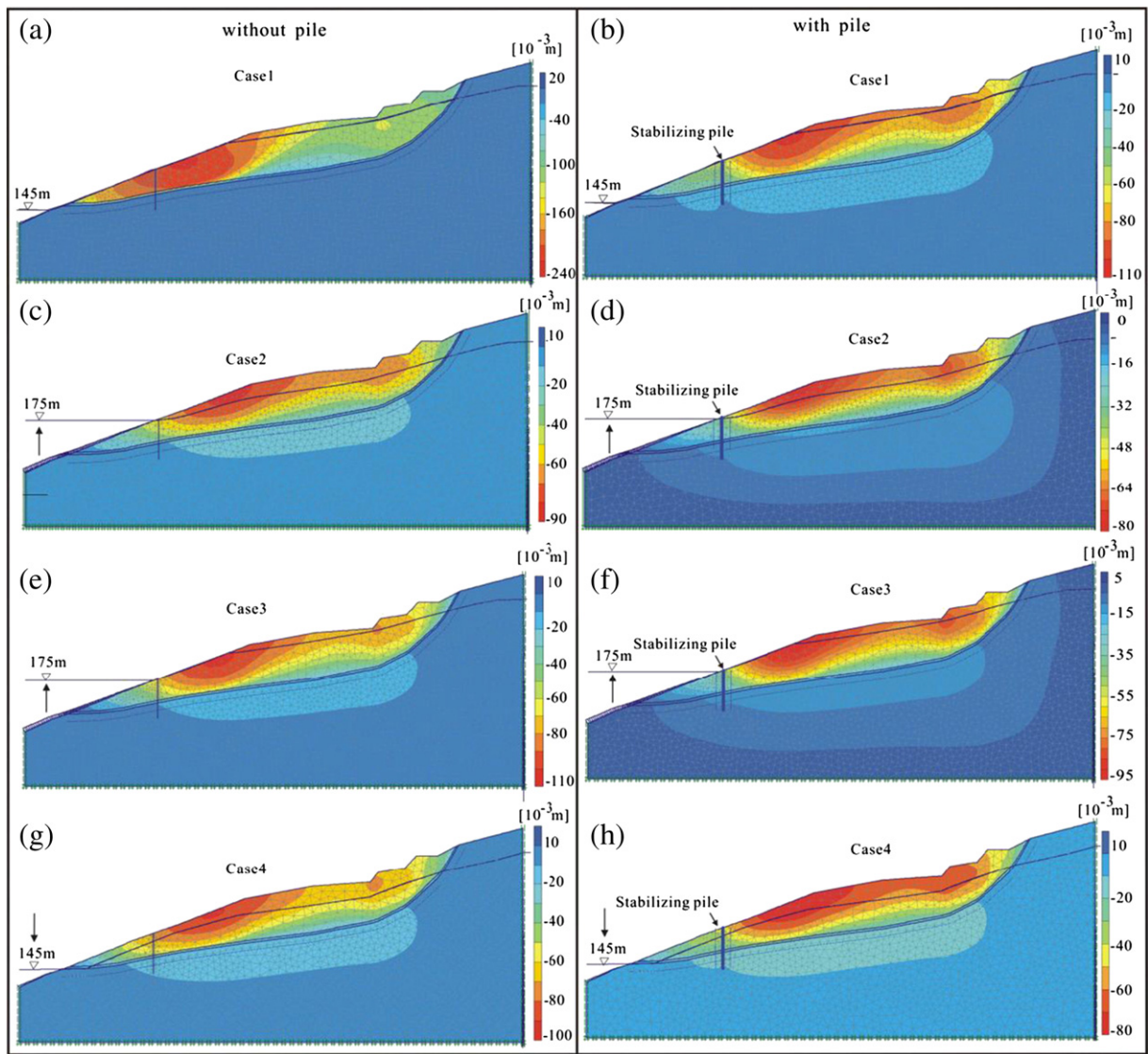


Fig. 12. The horizontal displacements of the landslide without the pile and with the pile separately. (a) and (b) are case 1: 145 m water level + rainfall amount of 360 mm/30-days; (c) and (d) are case 2: 175 m water level + rainfall amount of 150 mm/30-days; (e) and (f) are case 3: 175 m water level + rainfall amount of 360 mm/30-days; (g) and (h) are case 4: 175 m water level dropdown to 145 m water table + rainfall amount of 150 mm/30-days.

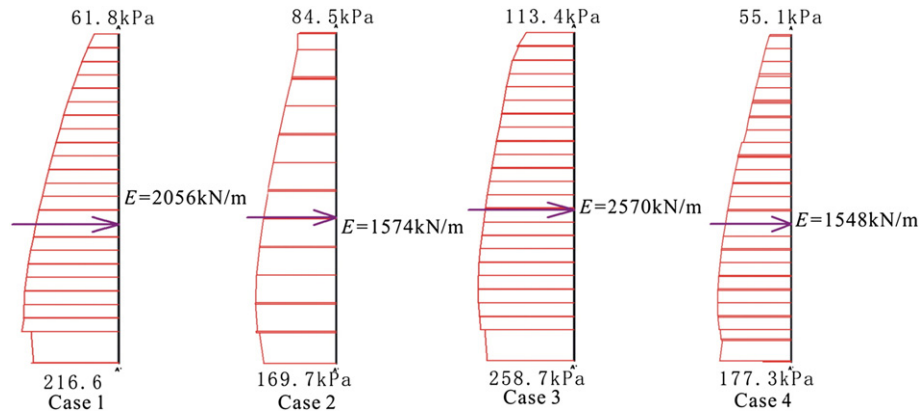


Fig. 13. The distribution of lateral force acting on the pile above the slip surface.

April to August (He et al., 2008). With the pile, the slope safety factor F_{s1}' increases and reaches to the desired slope safety factor 1.15. Comparing the two slope safety factors with and without the pile, we can conclude that the use of piles to stabilize the Ercengyan landslide can increase the slope safety factor, even with high water levels and high rainfall (case 3).

The lateral force E_{11} acting on the pile varies with the reservoir water level fluctuations and the rainfall amounts. When the reservoir water level rises to 175 m combined with a high rainfall amount (case 3), the lateral force acting on the pile E_{11} reaches to a peak of 2663 kN/m. However, when the reservoir water level rises to 175 m combined with a small rainfall amount (case 2), E_{11} falls to a minimum of 1487 kN/m. The lateral force is increased by 1176 kN/m because of the high rainfall amount (when comparing case 3 to case 2), and increased by 416 kN/m because of the high reservoir water level (when comparing case 3 to case 1).

The lateral force E_{11} acting on the pile is significantly influenced by the effective shear strength of the slip zone. A sensitivity analysis was carried out to determine the effect of shear strength on the lateral force (Figure 10). Based on the statistical analysis (see Section 2.3), we used the range of cohesion c to 10–40 kPa, and the friction angle ϕ to 10.5–18.5°. The lateral force E_{11} increases linearly as the cohesion c or friction angle ϕ of the slip zone decreases. When the cohesion c is constant, the lateral force E_{11} increases by 550 kN/m as ϕ decreases by 1°. And when the friction angle ϕ is constant, the lateral force E_{11} increases by 420 kN/m as c decreases by 3 kPa.

Ito and Matsui (1975) argue that the lateral force increases as c or ϕ increases because, when c or ϕ in the soil is larger, the soils just around and between the piles are harder to pass through, and hence the lateral

force becomes larger in a plastic state which satisfies Mohr–Coulomb's yield criterion. However, in this paper, we considered the soil at every 1 m width behind the pile, rather than the soil between the piles. The soil behind the pile is a rigid body and in a limit equilibrium state and, consequently, satisfies Mohr–Coulomb's yield criterion. These two viewpoints are reasonable due to different considerations. Practically, the conclusions from the LEM methods in this paper are more reliable for the design of the stabilizing pile in the Three Gorges Reservoir (Xu, 2012).

5.2. The lateral force modeling by the FE-SRM method

We modeled the slope geometry with a plane strain geometry model. The sliding soil, slip zone, and bedrock were simulated by an elastic–plastic model satisfying Mohr–Coulomb's yield criterion, and modeled using 15-node triangular elements. The properties of soil and rock appear in Table 1. The pile is considered as linear-elastic material and modeled using 5-node plate elements. The pile properties are given in Table 3. The model's x-direction had a width of 212 m, and its y-direction had a height of 91 m. It consisted of 6573 elements, 54,185 nodes and 78,876 stress points.

To model the suggested surface, a 1 m thick slip zone was considered along the slip surface (Figure 11). Between the slip zone and the bedrock, the first interface was used to model the movement of the slip zone along the bedrock while reducing the strength properties of the slip zone. The second interface around the pile was used to model the soil–pile interaction. The material properties of the interfaces are related to the adjacent soil, slip zone, and the bedrock elements. The

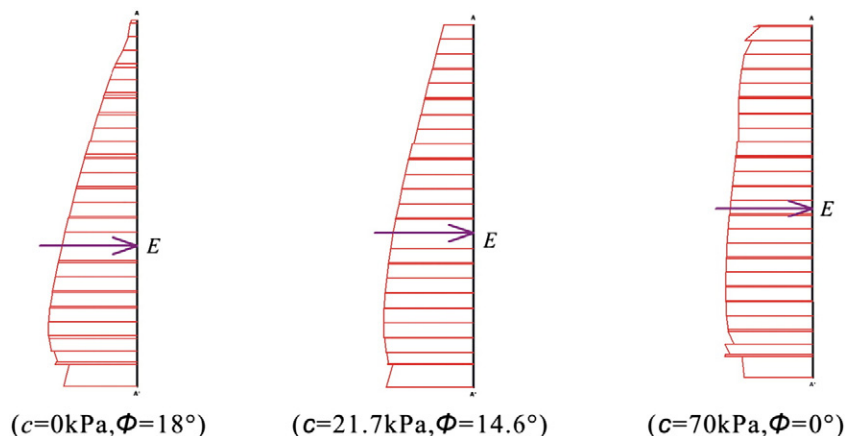


Fig. 14. Different distributions of lateral force with different shear strengths (case 4).

Table 4
Comparison of the LEM and FE-SRM methods ($c = 21.7 \text{ kPa}$, $\varphi = 14.6^\circ$).

Scenario	Slope Safety factor without pile F_{s1}		Lateral force E_{11} (kN)		Slope safety factor with pile F_{s1}'	
	LEM	FE-SRM	LEM	FE-SRM	LEM	FE-SRM
Case 1: 145 m water level + rainfall amount 360 mm (30-days)	0.99	1.05	2247	2056	1.18	1.17
Case 2: 175 m water level + rainfall amount 150 mm (30-days)	1.12	1.21	1487	1574	1.26	1.26
Case 3: 175 m water level + rainfall amount 360 mm (30-days)	1.01	1.03	2663	2570	1.26	1.25
Case 4: 175 m water level dropdown to 145 m water table + rainfall amount 150 mm (30-days)	1.07	1.13	1587	1548	1.21	1.20

decrease of strength was represented by a strength reduction factor $R_{int \text{ er}}$, which is shown in Table 1.

We simulated the landslide without the pile in the initial phase and with the pile in the next phase. Fig. 12 shows the horizontal displacements of the landslide without and with the pile. As demonstrated, the use of piles to stabilize the Ercengyan landslide can reduce the displacement of the sliding soil significantly, especially when water levels are lower and rainfall high (case 1). The displacements of the surface soil and pile were in agreement with the field measurements (Figure 12 b, d, f, and h).

The distribution of lateral force can be obtained from the normal stress distributions at the pile–soil interface above the slip surface. The models of lateral force distribution are approximate, following a parabolic distribution, with the peaks of lateral force near the surface

(Figure 13). The resultant force point of the lateral force is at $0.54\text{--}0.59 H_0$ (H_0 is the depth of the pile from ground surface to slip surface). The distributions of lateral force are consistent with the findings of Zheng and Zhao (2004) and Xu et al. (1988), who showed that the distribution of the lateral force acting on piles are parabolic as the ground surface behind the pile is inclined. The modeling for the distribution of the lateral force advances from the LEM method, such as in Hassiotis et al. (1997), with the assumption that the location of the maximum lateral force is at a distance of $1/3 H_0$.

The distribution of lateral forces acting on the stabilizing piles varies with the shear strength parameters of the slip zone (Figure 14). When the slip zone is a frictional soil ($c = 0$) in drained loading (Carter and Kulhawy, 1992), the distribution is approximately triangular. When the slip zone is made of colluvial and residual deposits, such as silty

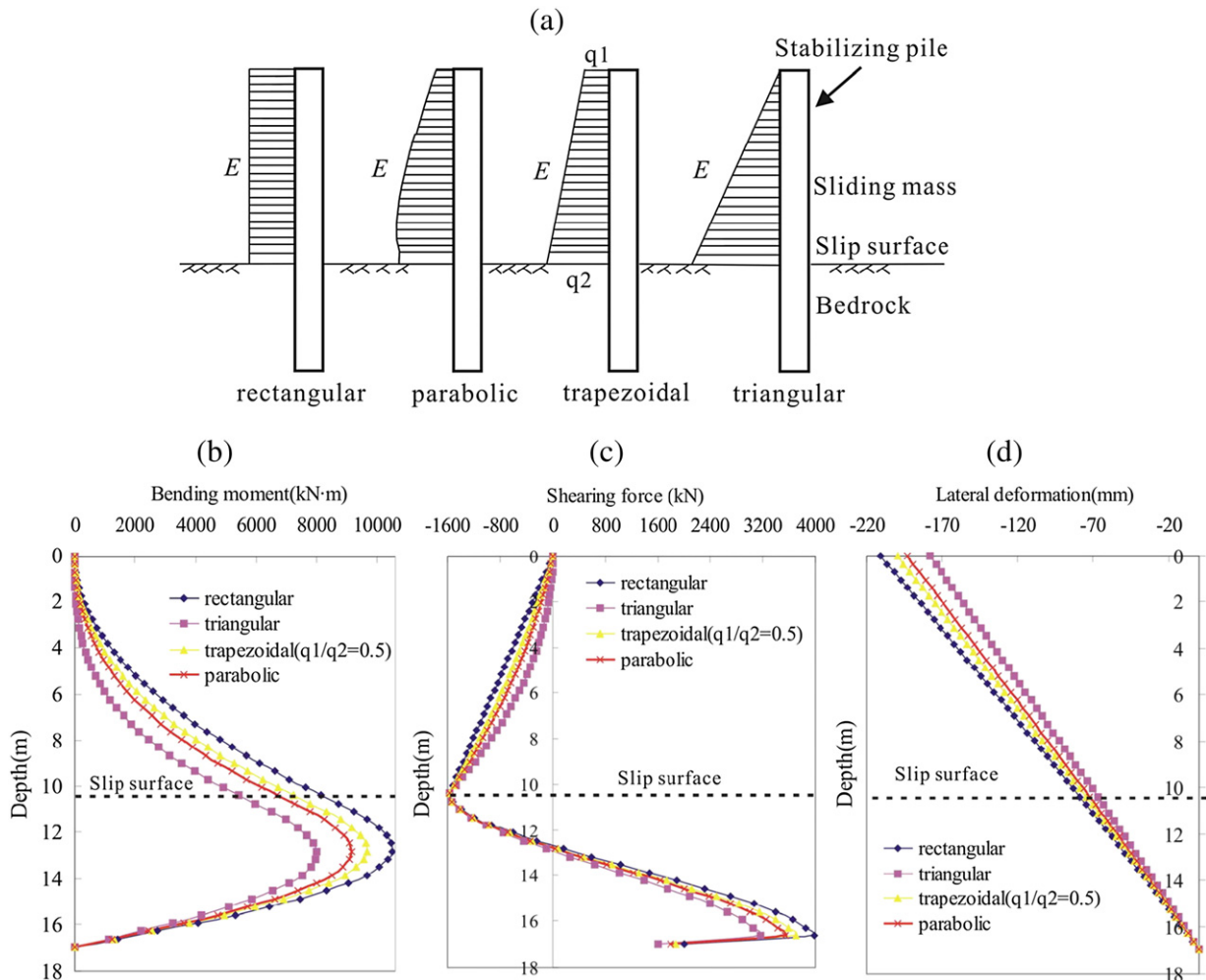


Fig. 15. Effect of the distribution of lateral force acting on the pile. (a) The parabolic distribution (FE-SRM method in this study), the traditional distribution: rectangular, trapezoidal and triangular; E is the lateral force for a 1 m-width of sliding soil (i.e., case 4) and $E = 1548 \text{ kN}$; the pile properties are given in Table 3, and the pile tip is hinged in the bedrock; (b) pile bending moment along pile depth; (c) shearing force along pile depth; (d) lateral deformation along pile depth.

clay with gravels, the distribution model is parabolic or trapezoidal. When the slip zone consists of cohesive soil ($\phi = 0$) in unstrained loading, the distribution is approximately rectangular. This conclusion is in agreement with both the TB 10025/J127 (2006) and the site measurements of the lateral force on the piles in other landslides.

6. Discussion and conclusions

The lateral forces from the LEM method are slightly larger than those from the FE-SRM method (Table 4), except for case 2. When the water level is high in the storage period and the rain amount is high (case 3), the lateral force by the LEM method is the maximum, larger by 191 kN than that by the FE-SRM method. The reasons for the difference, in addition to the studies by Cheng et al. (2007, 2008), are the different methods used to calculate the pore water pressure. In the LEM method, the interslice force for slices considers the seepage force of water acting on the direction of flow. Estimated by simplified methods in geotechnical engineering practice, the seepage force for the Ercengyan landslide is high when the reservoir water level is low and the rainfall amount high. However, in the FE-SRM method, steady-state pore water pressures and external water pressures are generated on the basis of phreatic levels (Brinkgreve and Vermeer, 2002). Flow pressure of pore water is low due to the pore water pressure remaining almost stable after 30-days of rainfall at a constant intensity (Figure 7).

The safety factors (F_{s1}) without the pile obtained from the FE-SRM method are slightly larger than those from the LEM method (Table 4). This result confirms the works by Cheng et al. (2007, 2008). Although there are some minor differences between the LEM and FE-SRM method in this example, the two methods for the stability analysis of landslide without and with the pile are, in general, satisfactory. We can calculate the lateral force and its distribution by the LEM and FE-SRM methods, and the results are consistent with field measurements.

The lateral forces acting on the pile are not constant, but dynamically changing with the reservoir water level fluctuations, rainfall amount, and effective shear strength of the slip zone. The lateral force and slope safety factor of the Ercengyan landslide are significantly influenced by the rainfall amount. When the reservoir water level rises to 175 m combined with high rainfall amount, the maximum lateral force is brought to act on the pile. The lateral force increases linearly as the shear strength of the slip zone decreases. Therefore, to reduce the risk of large-scale landslides, engineers should select the proper reservoir water level, rainfall amount, and effective shear strength of slip zone to get the lateral force when designing the stabilizing pile for extreme weather conditions.

The distributions of the lateral force change with the shear strength parameters of the slip zone. The distribution of the lateral force acting on the pile in the Ercengyan landslide approximately follows a parabolic distribution, and the resultant force point of the lateral force is at $0.54\text{--}0.59 H_0$ (H_0 is the depth of the pile from ground surface to slip surface). Different distributions of lateral force lead to the difference of pile lateral deformation, bending moment, and shearing force in the slope. Fig. 15a–d shows that when the distribution of lateral force is parabolic, the pile behavior (bending moment, shearing force, and lateral deformation) is smaller than the rectangular and trapezoidal distribution, and larger than the triangular distribution.

Acknowledgments

This research was funded by the National Natural Science Foundation of China (No. 41002112), the Natural Science Foundation of Hubei Province (No. 2010CDB11102), the China's Post-doctoral Science Fund (No. 20100480922), and the Science and Technology Project of Wuhan City (No. 201271031415). The authors would also like to thank D.G. Rossiter, Wouter van Heeswijk, Catherine Ann Lombard, and Thea Turkington and Xuanmei Fan for their valuable comments and suggestions for the improvement of the manuscript.

References

- Alonso, E.E., Pinyol, N.M., 2010. Criteria for rapid sliding I. A review of Vaiont case. *Eng. Geol.* 114, 198–210.
- Ashour, M., Ardan, H., 2012. Analysis of pile stabilized slopes based on soil–pile interaction. *Comput. Geotech.* 39, 85–97.
- Brinkgreve, R.B.J., Vermeer, P.A., 2002. *Plaxis Version 8 Reference Manual. Version 8.2* 2DBalkema Printers, Rotterdam, Netherlands 4.1–4.41.
- Brooks, R.H., Corey, A.T., 1964. Hydraulic properties of porous media. *Hydrology Papers Colorado State University* (March).
- Budhu, M., 1999. *Soil Mechanics and Foundations*. John Wiley & Sons, INCI, Berlin.
- Carter, J.P., Kulhawy, F.H., 1992. Analysis of laterally loaded shaft in rock. *J. Geotech. Geoenviron.* 839–855.
- Chen, D., 1999. Engineering geological problems in the Three Gorges Project on the Yangtze, China. *Eng. Geol.* 51, 183–193.
- Chen, L.T., Poulos, H.G., 1997. Piles subjected to lateral soil movements. *J. Geotech. Geoenviron.* 123, 802–811.
- Cheng, Y.M., Lansivaara, T., Wei, W.B., 2007. Two-dimensional slope stability analysis by limit equilibrium and strength reduction methods. *Comput. Geotech.* 34, 137–150.
- Cheng, Y.M., Lansivaara, T., Wei, W.B., 2008. Two-dimensional slope stability analysis by limit equilibrium and strength reduction methods: reply. *Comput. Geotech.* 35, 309–311.
- Chui, T.F.M., Freyberg, D.L., 2009. Implementing hydrologic boundary conditions in a multiphysics model. *J. Hydrol. Eng.* 14, 1374–1377.
- Cojean, R., Cai, Y.J., 2011. Analysis and modeling of slope stability in the Three-Gorges Dam reservoir (China)—the case of Huangtupo landslide. *J. Mt. Sci.* 8, 166–175.
- Comsol, A., 2013. *COMSOL Multiphysics User's Guide. Version* (July).
- Craig, R.F., 1987. *Soil Mechanics*, 4th edition. Van Nostrand Reinhold Co. Ltd., UK 88–98.
- Crosta, G.B., Frattini, P., 2008. Rainfall-induced landslides and debris flows—preface. *Hydrol. Process.* 22, 473–477.
- Gerscovich, D.M.S., Vargas Jr., E.A., de Campos, T.M.P., 2006. On the evaluation of unsaturated flow in a natural slope in Rio de Janeiro, Brazil. *Eng. Geol.* 88, 23–40.
- Griffiths, D.V., Lane, P.A., 1999. Slope stability analysis by finite elements. *Geotechnique* 49, 387–403.
- Hassiotis, S., Chameau, J.L., Gunaratne, M., 1997. Design method for stabilization of slopes with piles. *J. Geotech. Geoenviron.* 123, 314–323.
- He, K.Q., Li, X.R., Yan, X.Q., Guo, D., 2008. The landslides in the Three Gorges Reservoir Region, China and the effects of water storage and rain on their stability. *Environ. Geol.* 55, 55–63.
- Hendron Jr., A.J., Patton, F.D., 1987. The vaiont slide—a geotechnical analysis based on new geologic observations of the failure surface. *Eng. Geol.* 24, 475–491.
- Huang, R.Q., 2004. Mechanism of large scale landslides in western China. *Adv. Earth Sci.* 29, 443–450.
- Ito, T., Matsui, T., 1975. Methods to estimate lateral force acting on stabilizing piles. *Soil Found.* 15, 43–59.
- Ito, T., Matsui, T., Hong, W.P., 1981. Design method for stabilizing piles against landslide—one row of piles. *Soil Found.* 21, 21–37.
- Janbu, N., 1954. Application of composite slip surface for stability analysis. *Proceedings, European Conference on Stability of Earth Slopes*, 3, pp. 43–49 (Sweden).
- Jian, W.X., Yin, K.L., Yan, T.J., Cheng, C.J., 2005. Characteristics and formation mechanism of Minguochang landslide in Wanzhou District. *Chin. J. Geol. Hazard Control* 16 (4), 20–23 (in Chinese).
- Jian, W.X., Cheng, C.J., Yin, K.L., 2007. Primary investigation of characteristics and formation mechanism of Minguochang landslide. *1st North American Landslide Conference. Vail, Colorado, USA*, pp. 1628–1636 (June).
- Jian, W.X., Wang, Z.J., Yin, K.L., 2009. Mechanism of the Anlesi landslide in the Three Gorges Reservoir, China. *Eng. Geol.* 108, 86–95.
- Kahyaoglu, M.R., Onal, O., Imancli, G., Ozden, G., Kayalar, A.S., 2012. Soil arching load transfer mechanism for slope stabilized with piles. *J. Civ. Eng. Manag.* 18, 701–708.
- Kim, Y., Jeong, S., 2011. Analysis of soil resistance on laterally loaded piles based on 3D soil–pile interaction. *Comput. Geotech.* 38, 248–257.
- Kourkoulis, R., Gelagoti, F., Anastasopoulos, I., Gazetas, G., 2011. Slope stabilizing piles and pile-Groups: parametric study and design insights. *J. Geotech. Geoenviron.* 137, 663–677.
- Li, Y.Y., Yin, K.L., Chai, B., Zhang, G.R., 2008. Study on statistical rule of shear strength parameters of soil in landslide zone in Three Gorges Reservoir area. *Rock Soil Mech.* 29, 1419–1429.
- Liao, Q.L., Li, X., Lee, S., Dong, Y.H., 2005. Occurrence, geology and geomorphology characteristics and origin of Qianjiangping landslide in Three Gorges Reservoir area and study on ancient landslide criterion. *Chin. J. Rock Mech. Eng.* 24 (17), 3146–3153 (in Chinese).
- Lirer, S., 2012. Landslide stabilizing piles: experimental evidences and numerical interpretation. *Eng. Geol.* 149, 70–77.
- Luo, C., Yin, K.L., Chen, L.X., Jian, W.X., 2005. Strength parameters in sliding zone along horizontal-stratum landslides in Wanzhou City. *Chin. J. Rock Mech. Eng.* 24 (9), 1588–1593 (in Chinese).
- Morgenstern, N., 1965. The analysis of the stability of general slip surfaces. *Geotechnique* 15, 70–93.
- Poulos, H.G., 1995. Design of reinforcing piles to increase slope stability. *Can. Geotech. J.* 32, 808–818.
- Qiao, J., 2012. Landslide hazard prediction in the Three Gorges reservoir area, a case of reservoir bank in Wanzhou District, Chongqing City. *Science Publishing Company, Beijing* 20–21 (in Chinese).
- Rawls, W.J., Brakensiek, D.L., Saxton, K.E., 1982. Estimation of soil water properties. *Trans. ASAE* 25 (1916–1320), 1328.
- Robert, W.D., 1999. *Geotechnical and Foundation Engineering: Design and Construction*. R.R. Donnelley & Sons Company 10.14–10.15.

- Song, Y.S., Hong, W.P., Woo, K.S., 2012. Behavior and analysis of stabilizing piles installed in a cut slope during heavy rainfall. *Eng. Geol.* 129, 56–67.
- Spencer, E., 1967. A method of analysis of the stability of embankments assuming parallel interslice forces. *Geotechnique* 17, 11–26.
- TB 10025/J127, 2006. Code for design on retaining structures of railway subgrade. Standard of People's Republic of China (in Chinese).
- Van Asch, T.W.J., Malet, J.P., Van Beek, L.P.H., 2006. Influence of landslide geometry and kinematic deformation to describe the liquefaction of landslides: some theoretical considerations. *Eng. Geol.* 88, 59–69.
- Waltham, A.C., 1994. *Foundations of Engineering Geology*. Blackie academic & professional, Berlin.
- Wei, Z., Li, S., Wang, J.G., Wan, L., 2006. A dynamic comprehensive method for landslide control. *Eng. Geol.* 84, 1–11.
- Wen, B.P., Aydin, A., Duzgoren-Aydin, N.S., Li, Y.R., Chen, H.Y., Xiao, S.D., 2007. Residual strength of slip zones of large landslides in the Three Gorges area, China. *Eng. Geol.* 93, 82–98.
- Won, J., You, K.H., Jeong, S., Kim, S., 2005. Coupled effects in stability analysis of pile–slope systems. *Comput. Geotech.* 32, 304–315.
- Wu, S., Shi, L., Wang, R., Tan, C., Hu, D., Mei, Y., Xu, R., 2001. Zonation of the landslide hazards in the forereservoir region of the Three Gorges Project on the Yangtze River. *Eng. Geol.* 59, 51–58.
- Wu, F.Q., Luo, Y.H., Chang, Z.H., 2011. Slope reinforcement for housing in Three Gorges reservoir area. *J. Mt. Sci.* 8, 314–320.
- Xu, K.X., 2012. Technical requirements of design for geological disaster prevention project in the Three Gorges reservoir area. Command of Prevention and Control of Geological Disasters in Three Gorges Reservoir Area 25–40 (Yichang, in Chinese).
- Xu, L.D., Yin, D.C., Liu, H.M., 1988. Report of the first phase of model test of stabilizing pile—the distribution of lateral force acting on the pile. *Landslide CorpusChina Railway Publishing Company, Beijing* 25–28 (in Chinese).
- Yamin, M., Liang, R.Y., 2010. Limiting equilibrium method for slope/drilled shaft system. *Int. J. Numer. Anal. Methods Geomech.* 34, 1063–1075.
- Yu, J.T., 2005. Investigation Report of Ercengyan Landslide in Wanzhou District. Sichuan Huadi Building Engineering Co. Ltd., Chengdu 20–40 (in Chinese).
- Zhang, Y.M., Liu, G.R., Chang, H., 2004. Geological analysis of Qianjiangping landslide in Three Gorges Reservoir. *Yangtze River* 35 (9), 24–26 (in Chinese).
- Zheng, Y., Zhao, S., 2004. Calculation of inner force of support structure for landslide/slope by using strength reduction fem. *Chin. J. Rock Mech. Eng.* 23 (20), 3552–3558 (in Chinese).
- Zhou, C.M., 2007. Research on the design of anti-slide pile in Wan Zhou City of Three Gorges area. Ph.D dissertation of China University of Geosciences (Wuhan) 18–20 (Wuhan, in Chinese).
- Zhou, X.P., Cheng, H., 2013. Analysis of stability of three-dimensional slopes using the rigorous limit equilibrium method. *Eng. Geol.* 160, 21–33.
- Zhou, J., Xu, W., Yang, X., Shi, C., Yang, Z., 2010. The 28 October 1996 landslide and analysis of the stability of the current Huashiban slope at the Liangjiaren Hydropower Station, Southwest China. *Eng. Geol.* 114, 45–56.